THE JOURNAL OF PHYSICAL CHEMISTRY B

Article

pubs.acs.org/JPCB

Spectroscopic and Computational Study of Melittin, Cecropin A, and the Hybrid Peptide CM15

Diana E. Schlamadinger,[†] Yi Wang, J. Andrew McCammon, and Judy E. Kim*

Department of Chemistry and Biochemistry, University of California, San Diego, 9500 Gilman Drive, La Jolla, California 92093, United States

Supporting Information

ABSTRACT: Antimicrobial peptides (AMPs), such as cecropin A from silk moth, are key components of the innate immune system. They are effective defensive weapons against invading pathogens, yet they do not target host eukaryotic cells. In contrast, peptide toxins, such as honeybee melittin, are nondiscriminating and target both eukaryotic and prokaryotic cells. An AMP-toxin hybrid peptide that is composed of cecropin A and melittin (CM15) improves upon the antimicrobial activity of cecropin A without displaying the nonspecific, hemolytic properties of melittin. Here we report fluorescence and UV resonance Raman spectra of melittin, cecropin A, and CM15 with the goal of elucidating peptide-membrane interactions that help guide specificity. We have probed the potency for membrane disruption, local environment and structure of the single tryptophan residue, backbone conformation near the peptide hinge, and amide backbone structure of the peptides in lipid environments that mimic eukaryotic and prokaryotic membranes. These experimental results suggest that melittin inserts deeply into the bilayer, whereas cecropin A remains localized to the lipid headgroup region. A surprising finding is that CM15 is a potent membrane-disruptor despite its largely unfolded conformation. A molecular dynamics analysis complements these data and demonstrates the ability of CM15 to associate favorably with membranes as an unfolded peptide. This combined experimental−computational study suggests that new models for peptide−membrane interactions should be considered.

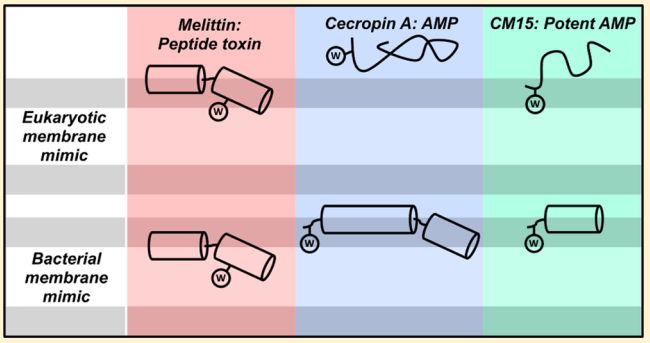

INTRODUCTION

Antimicrobial peptides (AMPs) are found in the animal and plant kingdoms and provide the first line of defense against invading pathogens. These peptides are a major component of the immune system of vertebrates and invertebrates and are especially critical for invertebrates, such as insects, that lack lymphocytes and antibodies.[1] In fact, the first AMPs to be isolated and purified were insect cecropins from silk moth *Hyalophora cecropia*.[2] Since this initial discovery from silk moth, cecropin peptides have been isolated from other insects as well as from mammals.[3,4] One of the most well-studied AMPs is the 37-residue peptide cecropin A, which exhibits broad-spectrum activity against certain bacteria yet remains relatively inactive against *Staphylococcus aureus*.[4] As with other AMPs, cecropin A shows minimal activity against eukaryotic cells and virtually no hemolytic activity.[5]

The activity of AMPs can be compared with that of nonspecific toxins. In contrast with AMPs, peptide toxins exhibit strong antimicrobial and hemolytic activity. Melittin is a well-studied 26-residue peptide toxin found in honeybee venom. Both melittin and cecropin A adopt amphipathic α-helical structures in organic solvents and in the presence of lipid membranes. One difference in structure is that melittin possesses hydrophobic N-terminal and basic C-terminal domains, whereas cecropin A exhibits the opposite motif and has basic N-terminal and hydrophobic C-terminal domains.[6] The single tryptophan residue of both peptides has been found to be critical for activity. Removal or substitution of the tryptophan residue in melittin causes a decrease in antimicrobial and hemolytic activity.[7,8] Substitution of the tryptophan residue in cecropin A also causes a significant decrease in antimicrobial activity;[9] however, replacement with a phenylalanine residue restores the activity.[10] Another striking similarity is that both melittin and cecropin A possess a single proline residue that gives rise to a flexible hinge region in the folded peptide. These flexible hinge regions have been reported to be important to the peptide activity.[11−13] Despite the commonalities in secondary structure, net charge, and key residues that contribute to peptide potency, these peptides possess remarkably different activities toward bacterial and eukaryotic cell types. For example, the potency against sheep red cells was found to be ∼100-fold greater for melittin than for cecropin A.[5]

Special Issue: Richard A. Mathies Festschrift

Received: April 25, 2012
Revised: July 10, 2012
Published: July 30, 2012

Table 1. Summary of Peptides[a]

peptide	function	primary sequence	net charge
melittin	toxin	GIGAVLKVLTTGLPALIS**W**IKRKRQQ	+6
cecropin A	AMP	KWKLFKKIEKVGQNIRDGIIKAGPAVAVVGQATQIAK	+7
CM15	potent AMP	KWKLFKKIGAVLKVL	+6

[a]Residues interrogated in the current report are highlighted in bold. Underlined portions of parent peptides constitute the sequence of amino acids present in the hybrid peptide CM15. The C-termini of all peptides are amidated.

Cecropin A and melittin often serve as templates in the construction of chimeric peptides that incorporate the best of both worlds: hybrid peptides are designed to retain the potency of toxins while exhibiting the selectivity and nonhemolytic behavior of AMPs.[14] In contrast with cecropin A, several hybrid peptides are active against the bacteria *Staphylococcus aureus*.[5] One such cecropin-melittin hybrid peptide consists of 15 residues from the N-terminal portions of cecropin A and melittin. This peptide, called CM15, is one of the shortest hybrids that exhibits improved antimicrobial activity relative to cecropin A.[5] CM15 is structurally similar to parent peptides in that it exhibits α-helical structure in solvents, micelles, and vesicles,[15−19] but it lacks a proline necessary for the flexible hinge region. CM15 preserves the high net positive charge of the parent peptides and retains the single tryptophan residue from cecropin A. Primary sequence and net charge of melittin, cecropin A, and CM15 are summarized in Table 1. CM15 provides a unique opportunity to investigate a synthetic peptide known for its potent antimicrobial activity and to also compare its biophysical properties to those of the parent peptides cecropin A and melittin.

Here we utilize electronic and vibrational spectroscopy combined with molecular dynamics (MD) simulations to probe melittin, cecropin A, and CM15 in different lipid environments. The local environment of the single tryptophan residue and secondary structures of the peptides were interrogated using UV resonance Raman (UVRR) spectroscopy and steady-state fluorescence. Peptide potency was evaluated using a leakage assay based on fluorescence of extrinsic dye molecules. The synthetic lipid bilayers are simple mimics of the membranes of eukaryotes (100% zwitterionic lipids) and prokaryotes (2:1 zwitterionic:anionic lipids). MD simulations of CM15 on the same lipid systems were also performed to complement these spectroscopic studies.

MATERIALS AND METHODS

Chemicals. Melittin, cecropin A, and CM15 were purchased from Axxora, Anaspec, and American Peptide Company, respectively. All peptides possess amidated C-termini in their native forms and were used as received. Anionic lipid 1-palmitoyl-2-oleoyl-*sn*-glycero-3-phospho-(1′-rac-glycerol) (sodium salt, POPG) and neutral lipid 1-palmitoyl-2-oleoyl-*sn*-glycero-3-phosphocholine (POPC) were purchased from Avanti Lipids in chloroform. Triton X-100 (TritonX) detergent was purchased from MP Biomedicals. Other chemicals and reagents were purchased from Fisher Scientific. Peptide concentrations for all experiments were 10−100 μM in 20 mM potassium phosphate buffer at pH 7.3. UVRR and fluorescence emission/anisotropy experiments were conducted on 40−50 μM peptide. Leakage assays were performed using the fluorophore 8-aminonaphthalene-1,3,6-trisulfonate (ANTS) and the quencher *p*-xylene-bis-pyridiniumbromide (DPX) from Invitrogen.

Vesicle Preparation. Anionic lipid vesicles were prepared by combining aliquots of POPC (10 mg) and POPG (5 mg) and drying the mixture under a stream of nitrogen. Zwitterionic lipid vesicles were prepared by omitting the POPG aliquot. Dried lipids were resuspended in phosphate buffer using a bath sonicator. For fluorophore/quencher containing vesicles, the buffer contained 50 mM ANTS and 50 mM DPX. Vesicles were prepared by extruding the lipid suspension thirteen times through a polycarbonate filter with pore size 200 nm using an extruder (EastSci). Vesicle solutions were filtered (0.45 μm membrane) and passed through a desalting column (10DG, BioRad). The first 3 mL elution was discarded, and the second 3 mL elution containing vesicles was collected and allowed to equilibrate at 37 °C. The final lipid concentration used in experiments was 1 mg/mL. All samples were incubated for 1 to 2 h at 37 °C prior to measurement.

Fluorescence Spectroscopy. Fluorescence spectra were acquired on a JobinYvon Horiba Fluorolog-3 spectrofluorometer. The excitation wavelength for tryptophan fluorescence was 290 nm, and the entrance and exit bandpass were 3.0 nm. Spectra of buffer with or without vesicles were subtracted from all raw peptide spectra. Steady-state anisotropy was measured by introducing vertical (V) and horizontal (H) polarizers in the excitation and emission paths. Fluorescence intensities I_{VV}, I_{VH}, I_{HH}, and I_{HV}, where the first and second subscripts refer to excitation and emission polarizations, respectively, were used to calculate the anisotropy.[20] The entrance bandpass and exit bandpass were 2.5 and 6.0 nm, respectively, for anisotropy experiments.

For leakage assay experiments, the excitation wavelength was 386 nm and the entrance bandpass and exit bandpass were 5.0 nm. TritonX detergent was added to ANTS/DPX-containing vesicle solutions to determine the maximum fluorescence intensity corresponding to 100% dye leakage.

UV Resonance Raman Spectroscopy. The UVRR setup has been described elsewhere.[21] In brief, vibrational spectra were obtained by setting the fundamental laser wavelength to 840 or 920 nm to generate 210 or 230 nm excitation beams, respectively. A typical sample volume of 2.0 mL was pumped through a vertically mounted fused silica capillary at a rate of 0.16 mL/min. The UV power was 3−5 mW at the sample. Ten 1 min spectra were collected and summed for all samples. UVRR spectra of appropriate blank solutions were also collected and subtracted from the corresponding raw peptide spectra. UVRR spectra presented here have been normalized to the most intense peak at ∼760 cm^{-1}. Accuracy and precision were determined using ethanol peaks and were found to be ±2 cm^{-1}. The bandpass for the Raman experiment was <11 cm^{-1}.

Molecular Dynamics Simulations. The CM15 peptide was simulated in a water box for 1 ns starting with a linear conformation. Ten representative structures of the peptide during the second half of this simulation were selected and used as initial structures in the peptide−lipid simulations. The peptide was placed in a box with two pre-equilibrated lipid

dx.doi.org/10.1021/jp304021t | J. Phys. Chem. B 2012, 116, 10600−10608

Table 2. Results from Tryptophan Fluorescence (λ_{max} and $r_{\lambda max}$), 230 and 210 nm UVRR Spectra (R_{W10}, R_{FD}, and folded %), and Leakage Assay with 30 μM Peptide (Leakage %) for Peptides in Buffer and in the Presence of Zwitterionic and Anionic Lipid Bilayers[a]

peptide	environment	λ_{max}	$r_{\lambda max}$	R_{W10}	R_{FD}	folded (%)	leakage (%)
melittin	buffer	355	0.02	1.5	1.2	*0*	
	zwitterionic	343	0.05	1.3	1.3	89	54
	anionic	336	0.07	1.2	1.7	97	46
	2 M NaCl	339	0.05	0.8	1.7	*100*	
cecropin A	buffer	356	0.02	1.6	1.0	*0*	
	zwitterionic	357	0.01	1.6	1.0	2	10
	anionic	340	0.08	2.8	1.3	*100*	67
CM15	buffer	358	0.02	1.5	1.0	*0*	
	zwitterionic	354	0.05	1.9	1.1	23	45
	anionic	343	0.09	3.2	1.4	*100*	24

[a]Values for melittin in 2 M NaCl are also reported. Italicized "folded (%)" values of 0 and 100% indicate selected basis spectra to represent unfolded and folded peptide for the UVRR fitting analysis. See the main text for details.

bilayers, one containing 78 POPC molecules and the other containing 52 POPC and 26 POPG molecules. CM15 was added to one side of the lipid bilayer, ~30 Å above the phosphorus atoms in the upper leaflet. To neutralize the net charge of the systems, we added 7 sodium and 13 chloride ions to the CM15-POPC system and 20 sodium ions to the CM15-POPC/POPG system. Ten 100 ns simulations were performed for each peptide−lipid system described above. The simulations were performed under the constant temperature, pressure, and surface area (NPAT) conditions with the program NAMD, release 2.7b1.[22] The simulation temperature was maintained at 300 K using Langevin dynamics, and the pressure was kept at 1 atm using a Nosé−Hoover−Langevin piston.[23] The CHARMM force field for proteins[24,25] and the latest update for lipids were utilized.[26] To improve the sampling efficiency, a soft boundary condition was applied to keep the peptide within 20 Å of the bilayer. When the peptide attempted to exit this 20 Å buffer zone, a weak restraining potential (spring constant 3 kcal/mol/Å^2) was applied to the center-of-mass of the peptide to prevent it from exiting the buffer zone. When the peptide was inside the buffer zone, however, no external force was applied, and the peptide diffused freely in bulk water or interacted with the lipid bilayer. Therefore, the effect of the soft boundary condition was an increase in sampling efficiency, which was achieved by keeping the peptide within the proximity of the bilayer without interfering with its inherent dynamics. In-depth simulation details and the effect of simulation ensembles are presented in a separate report.[27]

RESULTS

Fluorescence. Steady-state tryptophan fluorescence spectra were collected for each peptide in phosphate buffer, 100% POPC (zwitterionic) lipid vesicles, and 2:1 POPC:POPG (anionic) lipid vesicles. A tryptophan fluorescence spectrum of melittin in 2 M NaCl was also collected because it is known that melittin forms a folded α-helical soluble tetramer in a high salt environment.[28] The wavelength of maximum fluorescence emission (λ_{max}) and steady-state anisotropy at λ_{max} ($r_{\lambda max}$) for each peptide in the different environments are summarized in Table 2. The melittin tryptophan emission is blue-shifted 12, 19, and 16 nm in the presence of zwitterionic lipid vesicles, anionic lipid vesicles, and in 2 M NaCl, respectively, relative to its emission in phosphate buffer. The emission maximum of melittin in anionic lipid vesicles is the most blue-shifted fluorescence wavelength compared with the other peptide+lipid systems in this study. For cecropin A, the emission maximum blue-shifted only in the presence of anionic lipid vesicles. In contrast, the tryptophan emission of CM15 blue-shifted in both anionic lipid vesicles (−15 nm) and in zwitterionic lipid vesicles (−4 nm) relative to unfolded peptide.

The steady-state anisotropy of the tryptophan residue for each peptide correlates with the fluorescence results: the anisotropy, $r_{\lambda max}$, increased in environments that also caused blue shifts in emission. The anisotropy value of the tryptophan residue of CM15 also increased in zwitterionic lipid vesicles despite the relatively small shift in emission maximum.

Disruption of the synthetic lipid vesicle was measured using a fluorescence leakage assay.[29] The increase in ANTS fluorescence was monitored 1 h after the addition of peptides to vesicles with encapsulated ANTS/DPX mixture. The results of this assay are shown in Figure 1 as a percentage of leakage relative to the signal induced by the detergent TritonX. For ANTS/DPX-containing anionic lipid vesicles, cecropin A

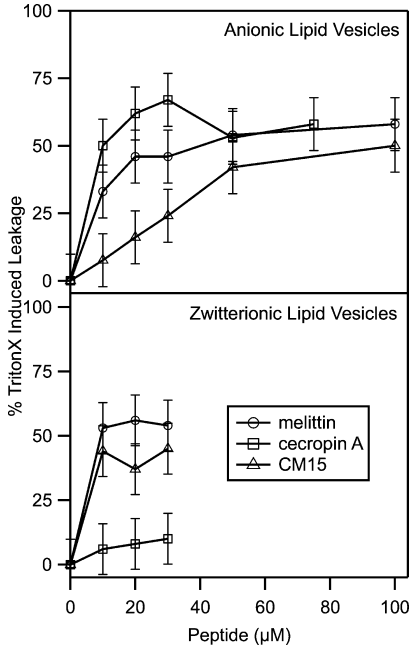

Figure 1. Leakage from anionic (top panel) and zwitterionic lipid vesicles (bottom panel) caused by melittin (circles), cecropin A (squares), and CM15 (triangles).

dx.doi.org/10.1021/jp304021t | J. Phys. Chem. B 2012, 116, 10600−10608

caused significant leakage at the lowest peptide concentration of 10 μM. The fluorescence signal quickly saturated at cecropin A and melittin concentrations of ~20 μM. CM15 did not cause significant leakage of anionic lipid vesicles at low peptide concentrations but was effective at peptide concentrations similar to those used in UVRR experiments (40 μM). A linear increase in leakage signal was observed up to 50 μM CM15.

Melittin and CM15 were potent against zwitterionic lipid vesicles and caused substantial leakage of the encapsulated ANTS/DPX. This leakage appeared to plateau after 10 μM peptide. As expected, cecropin A caused minimal leakage; in fact, the extent of leakage caused by cecropin A was similar to the leakage change observed when a tryptophan model compound, *N*-acetyl-L-tryptophanamide (NATA), was added to the vesicles (data not shown).

UVRR Spectroscopy. UVRR spectra with 230 nm excitation exhibit vibrational bands from the single tryptophan residue in each peptide. Figure 2 presents the W10 and W7

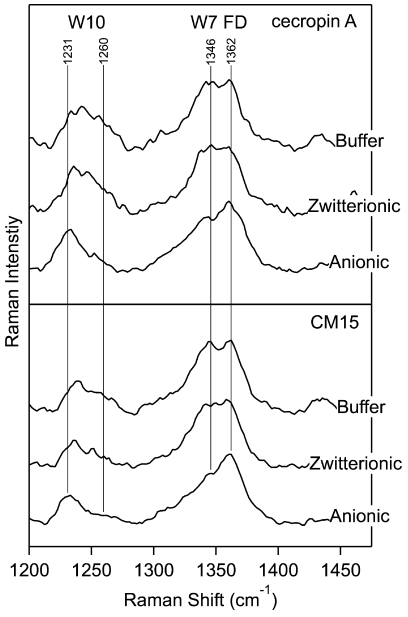

Figure 2. The W10 and W7 Fermi doublet (FD) regions in 230 nm UVRR spectra of cecropin A (top panel) and CM15 (bottom panel). In each panel, the spectra are of peptide in the presence of phosphate buffer (top), zwitterionic vesicles (middle), and anionic lipid vesicles (bottom).

Fermi doublet region of the 230 nm UVRR spectra of cecropin A and CM15 in phosphate buffer and in the presence of zwitterionic and anionic lipid vesicles. Expanded 230 nm UVRR spectra of cecropin A and CM15 are presented in Figure S1 (Supporting Information). UVRR spectra of melittin in phosphate buffer, 2 M NaCl, and anionic and zwitterionic lipid vesicles were presented and discussed in a previous publication.[30] The UVRR Fermi doublet intensity ratio (R_{FD} = I_{1362}/I_{1346}) and the W10 intensity ratio (R_{W10} = I_{W10}/I_{W9} = I_{1231}/I_{1260}) are reported in Table 2 for all peptides. R_{FD} and R_{W10} values were determined from the intensities of the bands at the indicated frequencies.

R_{FD} values for melittin increased in lipid and NaCl environments relative to in phosphate buffer. However, for cecropin A, the R_{FD} value increased only in the presence of anionic lipid vesicles. The R_{FD} value for CM15 increased significantly in the presence of anionic lipid vesicles and modestly in the presence of zwitterionic vesicles. For melittin, R_{W10} decreased in all lipid and salt environments relative to in buffer, with the lowest value in 2 M NaCl. Conversely, the R_{W10} value increased for cecropin A and CM15 bound to anionic lipid vesicles.

UVRR spectra with 210 nm excitation exhibit vibrational bands from the amide backbone. Figure 3 presents 210 nm

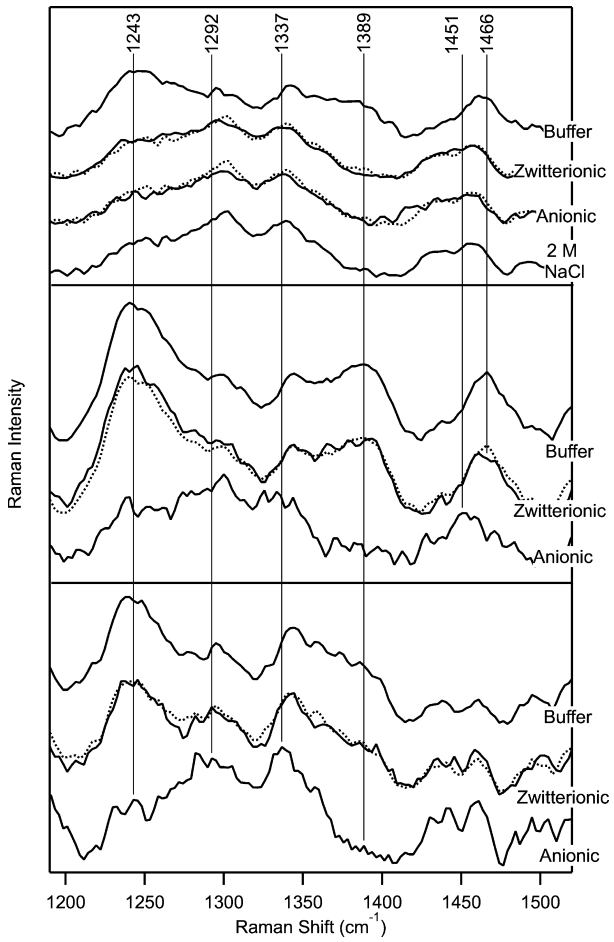

Figure 3. UVRR spectra with 210 nm excitation of melittin (top panel), cecropin A (middle panel), and CM15 (bottom panel). Dotted lines are resulting fits when basis spectra are composed of unfolded peptide in buffer and folded peptide in 2 M NaCl (melittin) or anionic lipids (cecropin A and CM15). See the text for details.

UVRR spectra in the region of amide III vibrations for melittin, cecropin A, and CM15 in the different lipid and salt environments. This region is sensitive to peptide secondary structure.[31−33] Significant changes in the amide III region are observed for melittin in 2 M NaCl and in the presence of lipid vesicles relative to melittin in phosphate buffer. Peaks near 1243 and 1389 cm^{-1} decrease in intensity, whereas the band near 1292 cm^{-1} increases in intensity when the peptide is bound to lipid or in 2 M NaCl. Analogous shifts in the amide III band are observed for cecropin A and CM15 in the presence of anionic lipid vesicles, but only minor or no UVRR changes are evident for these peptides in the presence of zwitterionic vesicles.

The amide IIp band (1440−1470 cm^{-1}) is prominent in spectra of peptides containing proline, such as melittin and cecropin A. A small band is also present in this region for CM15, which does not contain a proline residue. This band is

dx.doi.org/10.1021/jp304021t | J. Phys. Chem. B 2012, 116, 10600−10608

attributed to the trifluoroacetate counterion present in the CM15 sample obtained from the manufacturer.[34] For melittin, the amide IIp band downshifts from 1466 cm^{-1} and transforms into a doublet in the presence of lipid vesicles and 2 M NaCl. A similar shift is also observed in the spectrum of cecropin A in anionic lipid vesicles compared with the spectrum in phosphate buffer; however, it is unclear if the band evolves into a doublet based on the signal-to-noise ratio of this spectrum.

The percentage of secondary structure was determined by utilizing the fully folded and unfolded spectra as basis spectra; these basis spectra were summed to reproduce the observed spectrum. For melittin, the spectra of peptide in 2 M NaCl and in phosphate buffer served as the folded and unfolded basis spectra, respectively. The choice of the folded basis spectrum was based on previous experiments that established the soluble tetrameric form of melittin as a highly α-helical structure.[28] For cecropin A and CM15, the spectra in anionic lipid vesicles and in phosphate buffer were utilized as the folded and unfolded basis spectra, respectively. These basis spectra were selected based on similarity with the melittin folded basis spectrum and on circular dichroism experiments that indicated folded α-helical structures of cecropin A and CM15 in the presence of anionic lipid vesicles (Figure S2 of the Supporting Information).[16] The observed data were simulated with a sum of the basis spectra with variable coefficients via a least-squares fitting routine and are represented as dotted lines in Figure 3. The values are 89 and 97% folded for melittin in zwitterionic and anionic lipid vesicles, respectively. Cecropin A is 2% folded and CM15 is 23% folded in the presence of zwitterionic lipid vesicles. Percent folded values are summarized in Table 2.

Molecular Dynamics Simulations. Table 3 presents statistical analysis of key MD simulation results, including occurrences of CM15 insertion into the bilayer ("bilayer") or localization at the interfacial region ("interface") and average secondary structure content when the peptide inserted into the bilayer ("SS bilayer") or localized at the interface ("SS interface"). Values in the Table for "bilayer" and "interface" indicate the number of simulations (out of 10) that resulted in an occurrence of the specified event during the last 33 ns of the 100 ns simulation; an occurrence is given a value of "1" if the event persists beyond a threshold of 10% of the 33 ns window and a value of "0" if the event does not persist longer than the threshold period. The peptide was considered to be inserted in the bilayer if the center of mass of the peptide remained between the average levels of the upper and lower phosphorus atoms of the bilayer and was considered at the interface if it remained within 10 Å above or below the average levels of the upper and lower phosphorus atoms, respectively. The average levels of the upper (P_{upper}) and lower (P_{lower}) leaflet phosphorus atoms take into account the fluctuations in terms of the standard deviations of the phosphorus atoms (σ_{upper} and σ_{lower}). Therefore, "bilayer" is defined by the following condition, where Z_{com} is the location of the center of mass of the peptide: $P_{lower} - \sigma_{lower} < Z_{com} < P_{upper} + \sigma_{upper}$. Analogously, a peptide is considered to be at the lower leaflet interface when $P_{lower} - \sigma_{lower} - 10 < Z_{com} \leq P_{lower} - \sigma_{lower}$ and in the upper leaflet interface when $P_{upper} + \sigma_{upper} \leq Z_{com} < P_{upper} + \sigma_{upper} + 10$.

Table 3. Simulation Results[a]

vesicle type	bilayer	SS (bilayer)	interface	SS (interface)
zwitterionic lipids	1	0.00	5	0.20
anionic lipids	3	0.30	10	0.18

[a]Occurrences of CM15 insertion into the hydrocarbon bilayer ("bilayer") or localization at the interfacial region ("interface") and average secondary structure content within the bilayer ("SS bilayer") or at the interface ("SS interface"). See the text for details.

The extent of secondary structure, "SS bilayer" and "SS interface," reflects the average content of secondary structure when the peptide is inserted in the bilayer or localized at the interface. A value of "0" indicates that on average the peptide exhibited no α-helical structure. It should be noted that the results obtained from MD simulations reflect early events in peptide–lipid binding, and may vary from results obtained with longer simulation times. Nonetheless, differences are observed for CM15 in zwitterionic and anionic lipids, which allow comparison of peptide–lipid interactions in these two bilayers.

As expected, based on electrostatics, the cationic CM15 peptide interacted less frequently with the zwitterionic lipid bilayer relative to anionic lipids. For example, out of 10 total simulations, CM15 inserted into the zwitterionic bilayer ("bilayer") in one simulation and localized at the interfacial region ("interface") in five simulations. In contrast, CM15 inserted into the anionic bilayer in three simulations and localized at the interfacial region in all 10 simulations. Given the potential significance of the tryptophan residue, we also analyzed tryptophan burial in terms of the tryptophan center of mass and applied the same condition for insertion, as described for the peptide above. Tryptophan insertion in the zwitterionic lipid bilayer occurred in only one simulation, whereas this event occurred six times in the anionic lipid bilayer. Tryptophan trajectories of CM15 in the presence of zwitterionic and anionic lipid vesicles are presented in Figure S3 of the Supporting Information. In our expanded study that extended the MD simulations to 180 ns,[27] it was shown that the tryptophan residue of CM15 is in contact with anionic and zwitterionic lipid environments more frequently than any other residue of the peptide. In both lipid environments, there was a reduction in the fluctuations of the side-chain dihedral angle of the tryptophan residue (Figure S4 of the Supporting Information). As expected, the average number of salt bridges between lysine residues and lipids increased dramatically in the case of anionic lipids compared with the zwitterionic lipids, which is consistent with the presence of the negatively charged lipid POPG (data not shown).

In simulations that resulted in folding and insertion into the bilayer, the peptide assumed an orientation that is parallel to the bilayer; perpendicular orientations or bilayer traversal was not observed during the 100 ns simulation. In all peptide–lipid simulations, CM15 never folded into a perfectly helical structure (100%). One interesting, but unexpected, finding is that the peptide remained largely unfolded when it inserted into the zwitterionic bilayer. Snapshots of representative MD simulations of CM15 in the presence of zwitterionic and anionic lipid vesicles (t = 100 ns) are depicted in Figure 4. Electron density profiles generated from the lipid bilayer used for MD simulations are also presented with these snapshots.

DISCUSSION

Disruption of the Lipid Bilayer. Leakage assays are simple in vitro experiments that help reveal relative potencies of AMPs against different lipid compositions. Melittin causes leakage of both zwitterionic and anionic vesicles, supporting the previously reported nonspecific and potent activity toward bacterial and eukaryotic cells.[28] The leakage assay results for

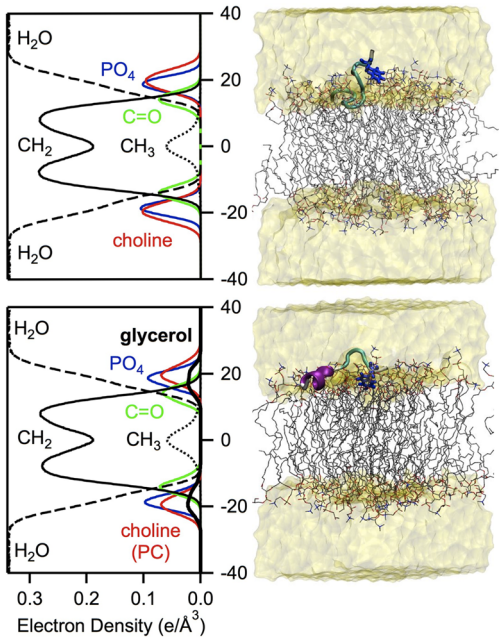

Figure 4. Results from MD simulations. Left: Electron densities of the bilayers composed of zwitterionic lipids (top) and anionic lipids (bottom). Right: Snapshots of CM15 in the presence of zwitterionic (top) and anionic (bottom) lipids. Colored regions of the peptide indicate α-helical structure (purple), turns (green), and random coil (black). The tryptophan residue is shown in blue.

cecropin A are also consistent with prior reports that this peptide is potent against bacterial, but not eukaryotic, cells.[5] CM15 gave a surprising result in that it disrupted zwitterionic lipid vesicles despite the known low level of hemolytic activity of this peptide.[5] This finding that CM15 affects the integrity of zwitterionic vesicles is consistent with leakage results previously reported for a similar cecropin-melittin hybrid peptide constructed from a longer section of melittin.[35] This prior study reported peptide concentration-dependent leakages for pure anionic and zwitterionic lipid vesicles that are similar to our results and showed that at low peptide concentrations, zwitterionic lipid vesicles leaked more than anionic lipid vesicles. These and our results indicate that cecropin−melittin hybrid peptides interact with both anionic and zwitterionic synthetic lipid vesicles.

Tryptophan Environment. The single tryptophan residue in melittin and cecropin is crucial for potency; omission of this residue significantly reduces peptide activity.[7,10] This tryptophan-associated potency may partially reflect the strong thermodynamic driving force of this residue for the bilayer.[36] Tryptophan fluorescence provides general insight, but the emission properties do not typically distinguish solvent polarity and hydrogen bonding of tryptophan residues.[20,30] In contrast, we previously reported that UVRR intensity ratios for different peaks are sensitive to local polarity (R_{FD}) or hydrogen bonding (R_{W10}) of tryptophan model compounds. For example, large R_{FD} values indicate a hydrophobic environment regardless of hydrogen bonding environment, and large R_{W10} values indicate strong hydrogen bonding of the N−H group regardless of local environment.[30] Here the low R_{FD} values and red-shifted fluorescence λ_{max} for the peptides unfolded in phosphate buffer indicate that the tryptophan residues are solvent-exposed (Table 2).[30]

The combined UVRR and fluorescence results reveal that the tryptophan residue of melittin inserts into both types of lipid vesicles studied here. Previously, we reported that the large fluorescence shift and high R_{FD} value in the case of melittin in the presence of anionic lipid vesicles is indicative of deep burial of tryptophan into the hydrocarbon core of the lipid bilayer.[30] This localization of the tryptophan residue is supported by low UVRR R_{W10} values that indicate minimal hydrogen bonding to lipid headgroups or water. The extent of burial into zwitterionic lipid vesicles is less than that into anionic lipid vesicles, evidenced by the systematic differences in fluorescence λ_{max}, anisotropy, and R_{FD} values for these two lipid systems.

The single tryptophan residue in CM15 originates from the cecropin A parent peptide, but the spectroscopic properties differ for CM15 and cecropin A. The fluorescence λ_{max}, anisotropy, and UVRR results for cecropin A in zwitterionic lipid vesicles are similar to those for the peptide in phosphate buffer; therefore, we conclude that the tryptophan residue in cecropin A does not interact with zwitterionic lipid vesicles. This lack of interaction is consistent with leakage assay results that indicate that cecropin A does not disrupt zwitterionic vesicles (Figure 1). The tryptophan residue of CM15 in the presence of zwitterionic lipid vesicles exhibits a more complex response. The subtle, but reproducible, shifts in fluorescence λ_{max} and UVRR intensity ratios indicate that this residue is not fully inserted into the lipid bilayer. However, these small spectral shifts indicate that there is measurable interaction between the tryptophan residue and the lipids. A similarly modest blue shift of tryptophan fluorescence for a longer cecropin−melittin hybrid peptide in the presence of zwitterionic lipid vesicles was also reported, further supporting our finding that the cecropin−melittin hybrid peptides interact with zwitterionic lipid vesicles in a subtle, but significant, manner.[35]

MD simulations corroborate these experimental findings; in simulations where W2 inserted into the bilayer, the tryptophan residue formed hydrogen bonds with the zwitterionic lipid head groups and was localized to ∼2 Å within the bilayer (data not shown). Furthermore, the simulations indicate that when tryptophan inserts into the bilayer, the orientation of the residue is motionally restricted (Figure S4 of the Supporting Information), and this finding is consistent with the experimentally observed increase in anisotropy in zwitterionic lipid vesicles. This tryptophan−lipid interaction may be partially responsible for the increased leakage observed for CM15 in the presence of zwitterionic lipid vesicles.

The enhanced R_{FD} values, blue-shifted λ_{max}, and increases in anisotropy for cecropin A and CM15 in the presence of anionic lipids support the insertion of tryptophan residues into these lipid vesicles. The tryptophan residue in CM15 and cecropin A also forms hydrogen bonds in anionic lipids; this interaction was not observed for melittin based on R_{W10} values in the UVRR spectrum (Table 2). These data suggest that tryptophan residues of cecropin and CM15 may not be buried as deeply in anionic lipid vesicles compared with melittin. We propose that CM15 and cecropin tryptophan residues are located close to the hydrogen-bond-accepting heteroatoms of the lipid headgroups because of the similarity of the intensity ratios (R_{FD} and R_{W10}) with previously reported values for tryptophan octyl ester (TOE), a model compound with a single interfacial tryptophan residue.[30,37]

MD simulations support the proposed location of the tryptophan residue of CM15 in anionic lipid bilayers. The tryptophan residue did not penetrate deeply into the

hydrocarbon core. Rather, it remained near the surface of the membrane in both zwitterionic and anionic lipid environments, as shown by their trajectories during the 100 ns simulation (Figure S3 of the Supporting Information). Furthermore, the indole N−H group formed hydrogen bonds with primarily the carbonyl and phosphate groups of the lipids. On average, the tryptophan residue of CM15 participated in hydrogen bonds more frequently in the case of anionic lipids than the zwitterionic lipids (data not shown); this finding is confirmed by the UVRR results, which indicated a greater R_{W10} intensity ratio in the presence of anionic lipid vesicles (Table 2). One reason for this enhanced hydrogen bonding in anionic lipids is because the anionic lipid possesses more hydrogen bond acceptors (two additional alcohol groups) than zwitterionic lipids. MD simulations also indicate that the CM15 tryptophan residue in anionic lipid vesicles is motionally restricted relative to in zwitterionic lipid vesicles, a finding that is consistent with experimental tryptophan anisotropy results (Figure S4 of the Supporting Information, Table 2).

Overall, the combined spectroscopic and MD simulation results suggest that deeply buried tryptophan residues may be characteristic of toxin−membrane interactions, whereas tryptophan residues that are localized and hydrogen-bonded to the interfacial region may reflect AMP−membrane interactions. Many factors contribute to the depth of burial for the tryptophan residue. One important consideration is the overall hydrophobicity of the peptide. Melittin is more hydrophobic than cecropin A, evidenced by GRAVY (grand average hydropathicity) values based on the Kyte and Doolittle hydropathy scale of 0.273 for melittin and −0.073 for cecropin A.[38] GRAVY values are calculated by summing hydropathy values for each amino acid and dividing by the number of residues in the sequence. A large GRAVY value indicates a hydrophobic sequence. The larger value calculated for melittin is consistent with the deep insertion of the tryptophan residue in lipid bilayers. However, a GRAVY value of 0.540 was calculated for CM15, indicating that overall peptide hydropathicity may play only a partial role in the tryptophan depth in lipid bilayers. In this case, the relatively short length of CM15 combined with its enhanced hydropathicity may allow it to adopt unfolded structures at the interface (see below).

The preference of tryptophan and other aromatic amino acids[39] for the interfacial region of bilayers is observed in different types of membrane proteins and peptides and suggests that tryptophan has functional relevance.[40] It has been postulated that tryptophan behaves as an anchor and orients the protein within the bilayer.[41] It has also been shown that tryptophan residues located in the interfacial region of the bilayer contribute to the overall thermodynamic stability of a membrane protein and play important functional roles in antibiotic channel peptides.[42,43] It has yet to be determined whether the tryptophan residue of CM15 is important for peptide activity. However, the spectroscopic and MD results discussed above suggest that the tryptophan residue of CM15 may play an important role in initiating peptide folding and insertion into the lipid bilayer. This conclusion is supported by the observation that the tryptophan residue interacts with both sets of lipids more often than any other CM15 residue according to the extended MD simulations.[27] Omission analogues or mutagenesis studies may provide additional insight into the importance of aromatic residues such as tryptophan in the primary sequence of engineered AMPs.

AMP Secondary Structure. The UVRR and CD spectra (Figure S2 of the Supporting Information) reveal secondary structure. The data indicate that all three peptides adopt random coil structure in buffer solution, evidenced by intense bands at 1243 and 1389 cm^{-1} and an upshifted amide IIp band at ∼1466 cm^{-1}.[31,44] The peptides adopt α-helical structure in the presence of anionic lipid vesicles (peaks at 1292 and 1337 cm^{-1} and absence of a band at 1389 cm^{-1}).[31,44] In the presence of zwitterionic vesicles, the peptides display variable structures: melittin is α-helical, cecropin A remains a random coil, and CM15 appears to retain partial secondary structure, discussed below.

Spectral fitting of the 210 nm UVRR spectrum of CM15 in zwitterionic lipid vesicles reveals that there is a minor contribution of folded signal (23%). We are unable to discern whether this contribution reflects a minor population of folded peptide or a dominant population of partially folded peptide. There is experimental evidence of the latter interpretation from a CD study that reported partial folding of CM15 in zwitterionic DMPC lipid vesicles.[16] Regardless of the origin of this minority signal of folded peptide, we conclude that CM15 interacts with and disrupts zwitterionic lipid vesicles in a primarily unfolded conformation.

Analysis of the 210 nm UVRR spectra includes investigation of the amide IIp doublet at 1440−1460 cm^{-1}. It has been suggested that this band is sensitive to protein conformation and hydrogen bonding, much like the bands that comprise the amide III region.[32] We previously quantified the doublet feature in melittin using the intensity ratio R_p, which is the ratio of intensities of the ∼1460 and ∼1440 cm^{-1} bands.[45] This analysis was based on the suggestion that the amide IIp band frequency is sensitive to hydrogen bonding of the leu-pro (melittin) carbonyl group. According to UVRR studies of dipeptides, frequencies near 1460 cm^{-1} are indicative of a strongly hydrogen bonded carbonyl, whereas frequencies near 1445 cm^{-1} represent minimal or no hydrogen bonding of the carbonyl group.[46] This interpretation is unlikely to be complete; a recent study reported that the amide IIp band frequency is not sensitive to hydrogen bonding but rather is a sensitive reporter of changes in the Ψ angle of the proline amide backbone.[47] Here we invoke both interpretations, with emphasis on the latter structure-based contribution.

Conformational analysis of the single proline residue and associated hinge region of melittin and cecropin A is important because the flexible hinge region has been found to be critical for peptide activity.[11−13] The amide IIp band in the spectrum of melittin downshifts in environments that induce folding, suggesting that the Ψ angle near the proline residue undergoes changes when the peptide assumes α-helical structure. In addition to this general downshift, the melittin amide IIp region becomes a doublet, indicating that the backbone near the proline residue may adopt two distinct orientations. These orientations may reflect two populations and are consistent with the crystal structure of tetrameric melittin, in which the proline Ψ angle takes on two different values for the four peptides. The amide IIp band for cecropin A in the presence of anionic lipid vesicles is more difficult to interpret because of the low signal-to-noise ratio. Nonetheless, it is clear that the amide IIp band also shifts to lower frequency for the folded peptide relative to unfolded cecropin A, consistent with structural changes associated with secondary structure formation.

In summary, the 210 nm UVRR results indicate that the secondary structure of melittin is not dependent on the type of

lipid environment utilized in this study. The structure of cecropin A and CM15, however, is dependent on the lipid environment. We also appreciate that the peptide structure may vary in the presence of natural eukaryotic or prokaryotic membranes.

The thermodynamics of partitioning is a critical factor in the structure of membrane-associated peptides. According to the White and Wimley hydrophobicity scale,[36] the free energy of partitioning CM15 from water to phosphatidylcholine lipids as an unfolded peptide is favorable, with a value of −1.87 kcal/mol. In contrast, ∼52% helix formation is required for cecropin A to have a total partitioning free energy of zero (7.65 kcal/mol for 0% helix formation and −7.15 kcal/mol for 100% helix formation), and the free energy for insertion of melittin in the unfolded state is around zero (−0.07 kcal/mol).[48] This calculation suggests that CM15 insertion into the phosphatidylcholine lipid bilayer may not require the formation of an α-helix and supports the experimental finding of a partially folded structure in zwitterionic lipids.

Disruption of membrane integrity in the presence of partially unfolded CM15 peptide may be caused by intermolecular hydrogen bonds. For example, groups within the amide backbone that would typically be hydrogen-bonded in the folded state may instead form favorable hydrogen bonds with lipid moieties. These interactions may disturb the integrity of the bilayer, causing the vesicle to leak. The presence of such hydrogen bonds is supported by the modest shift in R_{W10} in the appropriate direction (Table 2). It should be noted that CM15 does not exhibit hemolytic activity in in vivo assays,[5] indicating that the leakage assay utilized here does not provide a direct measure of peptide activity in red blood cells.

The observation that an unfolded peptide may be a potent membrane disruptor is not unprecedented. Previous studies on membrane-associated peptides reveal that secondary structure formation is not required for activity. Experiments incorporating D-amino acids into the primary sequence of peptides disrupted the α-helical secondary structure, but bactericidal activity was preserved.[49,50] Additionally, the single tryptophan residue of melittin diastereomers inserted into lipid vesicles despite the unfolded structure observed in helix-inducing solvents. Melittin diastereomers also caused leakage of dye-encapsulated vesicles. The results of experiments performed with membrane-active diastereomer peptides and CM15 in this work indicate that secondary structure may not be a prerequisite for the lytic activity of AMPs. This finding suggests that we should revisit and modify the commonly held belief that bilayer-disrupting peptides form secondary structure to be toxic.

CONCLUSIONS AND FUTURE OUTLOOK

Engineering robust and potent AMPs requires an in-depth understanding of molecular interactions between the peptide and lipid bilayer. Here we compare three membrane-associating peptides that have similar structure and net charge but display different selectivity and potency toward cells. Our findings indicate that a variety of molecular interactions are important to guide specificity and to improve potency in antimicrobial and toxic peptide−membrane interactions. In the case of CM15, for example, salt bridge formation between the cationic lysine residues and the negatively charged headgroups in anionic lipids occurs more often than with negative groups in zwitterionic lipids. We hypothesize that electrostatic interactions are responsible for initial peptide−membrane binding. However, the formation of salt bridges does not adequately explain the differences in peptide structure and potency reported here and elsewhere. Additional factors contribute to the specificity and potency of membrane-disruptive peptides, such as the position and insertion level of tryptophan or other aromatic residues, and overall peptide hydrophobicity. Lastly, secondary structure formation does not appear to be a necessary condition for peptide insertion into the bilayer or for bilayer disruption. This is an intriguing result that broadens our understanding of the mechanisms of action of these important peptides.

ASSOCIATED CONTENT

Supporting Information

Expanded 230 nm UVRR spectra of cecropin and CM15, CD spectra of all three peptides, trajectories and side-chain dihedral angles (from MD simulations) of the tryptophan residue of CM15 in zwitterionic and anionic lipid vesicles. This material is available free of charge via the Internet at http://pubs.acs.org.

AUTHOR INFORMATION

Corresponding Author

*E-mail: judyk@ucsd.edu. Tel: 858-534-8080. Fax: 858-534-7042.

Present Address

[†]Molecular Biophysics and Biochemistry Department, Yale University, 266 Whitney Avenue, P.O. Box 208114, New Haven, CT 06520.

Notes

The authors declare no competing financial interest.

ACKNOWLEDGMENTS

We thank Dina Kats for collection of steady-state anisotropy data and Dr. Yongxuan Su for assistance with CD spectroscopy. This study was supported by an NSF CAREER award to J.E.K. and a UCSD NIH Molecular Biophysics traineeship (GM 08326) to D.E.S. Projects in the McCammon group have been partially supported by NSF, NIH, Howard Hughes Medical Institute, Center for Theoretical Biological Physics, the National Biomedical Computation Resource, and the NSF supercomputer centers. The authors appreciate the computational resources provided by the Texas Advanced Computing Center (TG-MCA93S013 and TG-MCB100141). This research was also partially supported by the NSF through TeraGrid Supercomputer resources provided by a directors discretionary grant from the National Institute for Computational Science (TG-CHE100128) and the San Diego Supercomputer Center (TG-MCB090110) to Dr. Ross Walker.

REFERENCES

(1) Zasloff, M. *Nature* **2002**, *415*, 389−395.
(2) Brogden, K. A. *Nat. Rev. Microbiol.* **2005**, *3*, 238−250.
(3) Steiner, H.; Hultmark, D.; Engström, Å.; Bennich, H.; Boman, H. G. *Nature* **1981**, *292*, 246−248.
(4) Sato, H.; Feix, J. B. *Biochim. Biophys. Acta* **2006**, *1758*, 1245−1256.
(5) Andreu, D.; Ubach, J.; Boman, A.; Wåhlin, B.; Wade, D.; Merrifield, R. B.; Boman, H. G. *FEBS Lett.* **1992**, *296*, 190−194.
(6) Bechinger, B. *J. Membr. Biol.* **1997**, *156*, 197−211.
(7) Blondelle, S. E.; Houghten, R. A. *Biochemistry* **1991**, *30*, 4671−4678.
(8) Blondelle, S. E.; Houghten, R. A. *Peptide Res.* **1991**, *4*, 12−18.

(9) Andreu, D.; Merrifield, R. B.; Steiner, H.; Boman, H. G. *Biochemistry* **1985**, *24*, 1683−1688.
(10) Andreu, D.; Merrifield, R. B.; Steiner, H.; Boman, H. G. *Proc. Natl. Acad. Sci. U.S.A.* **1983**, *80*, 6475−6479.
(11) Fink, J.; Boman, A.; Boman, H. G.; Merrifield, R. B. *Int. J. Pept. Protein Res.* **1989**, *33*, 412−421.
(12) Rex, S. *Biophys. Chem.* **2000**, *85*, 209−228.
(13) Dempsey, C. E.; Bazzo, R.; Harvey, T. S.; Syperek, I.; Boheim, G.; Campbell, I. D. *FEBS Lett.* **1991**, *281*, 240−244.
(14) Rivas, L.; Andreu, D. In *Pore-Forming Peptides and Protein Toxins*; Menestrina, G., Serra, M. D., Lazarovici, P., Eds.; Taylor and Francis, Inc.: New York, 2003.
(15) Respondek, M.; Madl, T.; Göbl, C.; Golser, R.; Zangger, K. *J. Am. Chem. Soc.* **2007**, *129*, 5228−5234.
(16) Abrunhosa, F.; Faria, S.; Gomes, P.; Tomaz, I.; Pessoa, J. C.; Andreu, D.; Bastos, M. *J. Phys. Chem. B* **2005**, *109*, 17311−17319.
(17) Fernández, I.; Ubach, J.; Fuxreiter, M.; Andreu, J. M.; Andreu, D.; Pons, M. *Chem.—Eur. J.* **1996**, *2*, 838−846.
(18) McMahon, H. A.; Alfieri, K. N.; Clark, K. A. A.; Londergan, C. H. *J. Phys. Chem. Lett.* **2010**, *1*, 850−855.
(19) Alfieri, K. N.; Vienneau, A. R.; Londergan, C. H. *Biochemistry* **2011**, *50*, 11097−11108.
(20) Lakowicz, J. R. *Principles of Fluorescence Spectroscopy*, 3rd ed.; Springer: New York, 2006.
(21) Sanchez, K. M.; Neary, T. J.; Kim, J. E. *J. Phys. Chem. B* **2008**, *112*, 9507−9511.
(22) Phillips, J. C.; Braun, R.; Wang, W.; Gumbart, J.; Tajkhorshid, E.; Villa, E.; Chipot, C.; Skeel, R. D.; Kalé, L.; Schulten, K. *J. Comput. Chem.* **2005**, *26*, 1781−1802.
(23) Feller, S. E.; Zhang, Y.; Pastor, R. W.; Brooks, B. R. *J. Chem. Phys.* **1995**, *103*, 4613−4621.
(24) MacKerell, A. D., Jr.; Bashforde, D.; Bellott, M.; Dunbrack, R. L.; Evanseck, J. D.; Field, M. J.; Fischer, S.; Gao, J.; Guo, H.; Ha, S.; Joseph, D.; Kuchnir, L.; Kuczera, K.; Lau, F. T. K.; Mattos, C.; Michnick, S.; Ngo, T.; Nguyen, D. T.; Prodhom, B.; Reiher, I. W. E.; Roux, B.; Schlenkrich, M.; Smith, J.; Stote, R.; Straub, J.; Watanabe, M.; Wiorkiewicz-Kuczera, J.; Yin, D.; Karplus, M. *J. Phys. Chem. B* **1998**, *102*, 3586−3616.
(25) Mackerell, A. D.; Feig, M.; Brooks, C. L. *J. Comput. Chem.* **2004**, *25*, 1400−1415.
(26) Klauda, J. B.; Venable, R. M.; Freites, J. A.; O'Connor, J. W.; Tobias, D. J.; Mondragon-Ramirez, C.; Vorobyov, I.; Mackerell, A. D.; Pastor, R. W. *J. Phys. Chem. B* **2010**, *114*, 7830−7843.
(27) Wang, Y.; Schlamadinger, D. E.; Kim, J. E.; McCammon, J. A. *Biochim. Biophys. Acta, Biomembr.* **2012**, *1818*, 1402−1409.
(28) Raghuraman, H.; Chattopadhyay, A. *Biosci. Rep.* **2006**, *27*, 189−223.
(29) Ellens, H.; Bentz, J.; Szoka, F. C. *Biochemistry* **1984**, *23*, 1532−1538.
(30) Schlamadinger, D. E.; Gable, J. E.; Kim, J. E. *J. Phys. Chem. B* **2009**, *113*, 14769−14778.
(31) Huang, C.-Y.; Balakrishnan, G.; Spiro, T. G. *J. Raman Spectrosc.* **2006**, *37*, 277−282.
(32) Caswell, D. S.; Spiro, T. G. *J. Am. Chem. Soc.* **1987**, *109*, 2796−2800.
(33) Asher, S. A.; Ianoul, A.; Mix, G.; Boyden, M. N.; Karnoup, A.; Diem, M.; Schweitzer-Stenner, R. *J. Am. Chem. Soc.* **2001**, *123*, 11775−11781.
(34) Dreaden, T. M.; Chen, J.; Rexroth, S.; Barry, B. A. *J. Biol. Chem.* **2011**, *286*, 22632−22641.
(35) Mancheño, J. M.; Oñaderra, M.; Martínez del Pozo, A.; Díaz-Achirica, P.; Andreu, D.; Rivas, L.; Gavilanes, J. G. *Biochemistry* **1996**, *35*, 9892−9899.
(36) Wimley, W. C.; White, S. H. *Nat. Struct. Biol.* **1996**, *3*, 842−848.
(37) Ladokhin, A. S.; Holloway, P. W. *Biophys. J.* **1995**, *69*, 506−517.
(38) Kyte, J.; Doolittle, R. F. *J. Mol. Biol.* **1982**, *157*, 105−132.
(39) Sul, S.; Feng, Y.; Le, U.; Tobias, D. J.; Ge, N.-H. *J. Phys. Chem. B* **2010**, *114*, 1180−1190.
(40) White, S. H.; Wimley, W. C. *Annu. Rev. Biophys. Biomol. Struct.* **1999**, *28*, 319−365.
(41) Killian, J. A.; von Heijne, G. *Trends Biochem. Sci.* **2000**, *25*, 429−434.
(42) Sanchez, K. M.; Gable, J. E.; Schlamadinger, D. E.; Kim, J. E. *Biochemistry* **2008**, *47*, 12844−12852.
(43) Becker, M. D.; Greathouse, D. V.; Koeppe, R. E.; Andersen, O. S. *Biochemistry* **1991**, *30*, 8830−8839.
(44) Chi, Z.; Chen, X. G.; Holtz, J. S.; Asher, S. A. *Biochemistry* **1998**, *37*, 2854−2864.
(45) Schlamadinger, D. E.; Gable, J. E.; Kim, J. E. *Proc. SPIE* **2009**, *7397*, 73970J−1−73970J−13.
(46) Jordan, T.; Mukerji, I.; Wang, Y.; Spiro, T. G. *J. Mol. Struct.* **1996**, *379*, 51−64.
(47) Ahmed, Z.; Myshakina, N. S.; Asher, S. A. *J. Phys. Chem. B* **2009**, *113*, 11252−11259.
(48) Snider, C.; Jayasinghe, S.; Hristova, K.; White, S. H. *Protein Sci.* **2009**, *18*, 2624−2628.
(49) Oren, Z.; Shai, Y. *Biochemistry* **1997**, *36*, 1826−1835.
(50) Oren, Z.; Shai, Y. *Eur. J. Biochem.* **1996**, *237*, 303−310.